

NUMERICAL SOLUTION OF TWO-REGION ADVECTION-DISPERSION TRANSPORT AND COMPARISON WITH ANALYTICAL SOLUTION ON EXAMPLE PROBLEMS *

MILAN HOKR AND JIŘÍ MARYŠKA †

Abstract. We deal with a two-region porous media transport, which represent either solute transport in a medium with immobile pore zone (double or dual porosity) or solute transport with nonequilibrium sorption. The model consist of two coupled PDEs for mobile and immobile zone. Numerical solution is based on the finite volume method, with explicit upstream scheme for advection term and analytical solution of ODE representing the exchange between mobile and immobile zone. For suitable 1D problem, with exactly solved plain advection-dispersion problem, we show that after involving the effect of mobile-immobile exchange, the numerical solution is very close to the analytical solution. The results in example cases give a groundwork information for a use of the model for realistic problems.

Key words. nonequilibrium transport, porous media, advection-dispersion equation

AMS subject classifications. 65P05, 76R99, 76S05

1. Introduction. The development of the model is motivated by the problem of remediation of underground water after finishing the chemical mining activity in Stráž pod Ralskem region. In the case of remediation, in comparison with the mining itself, different physical and chemical processes have predominate influence to the contaminant transport. One of the phenomena, which now needs to be included to the used contaminant transport model, is the effect of immobile pore zone, in other words blind pores, which contain contaminated solution, but can not be cleaned instantly by moving water – the contaminants first diffuse to the zone with mobile water and then they are removed. This effect is well observed on curves of time development of concentration measured in pumping wells – the curve has a characteristic “tail”, it does not fall to zero as quickly as in the case without the immobile zone. Correct predictions of the drawn solute concentration are very important for planning the industrial processing of the produced solution.

The presented numerical approach, based on explicit upstream scheme, differs from models common in the literature. Although there is a complicated control of the accuracy of dispersion calculation, the model gives reasonable results for practical problems (in e.g. [4], concerning the model without the effect of non-equilibrium exchange). In this paper, we focus on the numerical modelling of the non-equilibrium exchange and we consider the advection-dispersion model under such conditions that the given physical problem can be solved (i.e. the discretisation is appropriate and the dispersion coefficient is in the specified limits (3.2)).

2. Physical and numerical model. The problem of solute transport in porous media is governed by the advection-dispersion equation. The solute transport in media with distinct mobile and immobile zones (dual-porosity media) can be described by two-region model, first proposed in [2]. We consider two field of concentration $c_m(\mathbf{x}, t)$

*This work was supported by Grant No.: 105/00/1089 (GAČR).

†Department of Modelling of Processes, Faculty of Mechatronics, Technical University of Liberec, Hálkova 6, 46117 Liberec, Czech Republic (milan.hokr@vslib.cz).

and $c_i(\mathbf{x}, t)$ in the same computational domain, they represent the concentrations in the mobile and immobile part (porosities n_m and n_i) of the representative volume. The concentration in the immobile zone is influenced only by the exchange with the mobile zone. The rate of exchange is assumed to be linear on the concentration difference, with a coefficient α . The exchange enter the advection-dispersion equation for the mobile zone as an additional source-sink term. The above is expressed by the following system of equations

$$(2.1) \quad \frac{\partial c_m}{\partial t} + \nabla(\mathbf{v} \cdot c_m) - \nabla \cdot (D \nabla c_m) = c^* q_s^+ + c_m q_s^- + \frac{1}{n_m} \alpha (c_i - c_m),$$

$$(2.2) \quad \frac{\partial c_i}{\partial t} = -\frac{1}{n_i} \alpha (c_i - c_m),$$

where c_m, c_i are the above mentioned concentrations (unknowns), \mathbf{v} is the seepage velocity, D is the dispersion coefficient (scalar), $q_s^+ > 0$ is the fluid source intensity, $q_s^- < 0$ is the fluid sink intensity and c^* is the given injected solute concentration.

2.1. Models of flow and transport. Besides directly entered input parameters as e.g. porosity and initial and boundary conditions, the transport model needs the field of the velocity $\mathbf{v}(\mathbf{x}, t)$, a solution of Darcy-Law-flow model, to be given. The flow field is not a subject of this paper, we just mention some important features.

The discretisations in flow and transport models are closely related to each other. We used a mixed-hybrid finite element approximation of the flow problem, governed by the Darcy Law and the mass balance equation [1]. The mathematical formulation of the model and its numerical properties are presented in [5]. As the outputs, the model provides values of pressure in element centers, values of pressure in side centers and fluxes through interelement sides. Using the same geometrical discretisation and the advection-calculation scheme (2.3) described below, we can use directly the value of interelement flux in the place of velocity.

The practical implementation of the flow and transport model use trilateral prismatic elements, which are suitable for discretising layered geological structures and convenient in algorithmical processing, because the mesh is not fully unstructured in 3D. Here presented numerical principles are independent on the element and volume shapes and the equations are expressed in more general form.

2.2. Principles of the numerical solution. The transport in the mobile zone is solved by the finite volume method (FVM) with the volumes geometrically identical to the elements of the fluid flow model. We use a time-explicit scheme and we consider the operator splitting for the approximation of the terms in the equation (2.1). In certain time step, the advection is calculated (2.3) and then the exchange between the mobile and immobile zone during is performed (2.8). The dispersion is not explicitly incorporated into the numerical method, but our experience confirm that the real dispersion can be roughly compensated by the numerical dispersion of the upstream approximation of the advection term. The conditions for this assumption are discussed in the section 3, the coefficient of the physical dispersion D and the mesh and time step must be in the relation $D \approx \frac{1}{2} v \Delta x$ and $C_r \ll 1$ (see below). It is possible to match measurement results in practical calculations on naturally constructed meshes.

The limitations posed on dispersion calculation in the discussed model are a charge for the less computational cost of the model: The explicit scheme for dispersion calculation require a stronger stability condition on Δt and thus a markedly higher number of time steps. The various types of implicit formulation, usually mentioned in the literature as a solution method for porous media transport, require a solution of a large

non-symmetric matrix in each time step. The approaches of incorporating the non-equilibrium exchange to an implicit-scheme model are discussed in [3] and compared with a solution through discretisation of Laplace-transformed problem, which also leads to a non-symmetric algebraic system.

2.3. Scheme and stability condition for advection. We use the following scheme with cell-centered values of concentration in the mobile zone

$$(2.3) \quad C_k^{n+1} = C_k^n + \frac{\Delta t}{V_k} \cdot \left[- \sum_{j \in N_k} (U_{kj}^+ C_k^n + U_{kj}^- C_j^n) + C_k^n Q_k^- + \tilde{C}_k^n Q_k^+ \right],$$

where in the k -th cell: C_k^n is the value of (mobile) concentration in the n -th time step (in time $t = n\Delta t$), Q_k is the source/sink intensity of fluid, \tilde{C}_k^n is the injected concentration (given), V_k is the volume of the cell, N_k is the index set of neighbour cells. Next, U_{kj} are the fluxes from k -th cell to j -th cell, and the superscripts $+$ and $-$ denote a positive and negative “part” of a number ($a^+ = a$ for $a \geq 0$ and $a^+ = 0$ for $a < 0$ etc.). We remark, that thanks to the properties of the mixed-hybrid flow model, the relation $U_{kj} = -U_{jk}$ automatically holds and thus the discretised transport model keeps the mass-balance of the transported solute.

The stability condition for the scheme is

$$(2.4) \quad \Delta t \sum_{j \in N_k} U_{kj}^+ \leq V_k \quad \text{and} \quad \Delta t \sum_{j \in N_k} (-U_{kj}^-) \leq V_k \quad \forall k,$$

which is a form of the well-known 1D condition $C_r = \frac{v\Delta t}{\Delta x} \leq 1$ (CFL condition), where C_r is the Courant number. This is a restrictive condition on the time step, which must not exceed certain value, depending on the mesh and the velocity field. The practical compliance of the condition is performed by successive halving of user-given time step, until the condition (2.4) in all the discretisation volumes is fulfilled.

2.4. Calculation of the mobile-immobile exchange. For expression of the exchange term, we derived a semi-analytical method. The operator splitting in the system (2.1)-(2.2) leads to a solution of two coupled ODE in a given space point (or discretisation volume) in each time step

$$(2.5) \quad \frac{dc_m}{dt} = \frac{1}{n_m} \alpha (c_i - c_m),$$

$$(2.6) \quad \frac{dc_i}{dt} = -\frac{1}{n_i} \alpha (c_i - c_m),$$

which honour the mass balance $n_m c_m + n_i c_i = \text{const}$. The exact solution of (2.5)-(2.6) for arbitrary time $t \geq 0$ is

$$(2.7) \quad c_m(t) = (c_m^{(0)} - \bar{c}^{(0)}) e^{-\alpha \frac{n_m + n_i}{n_m n_i} t} + \bar{c}^{(0)}$$

and by analogy for $c_i(t)$. We denoted $c_m^{(0)}$ and $\bar{c}^{(0)} = \frac{n_m c_m + n_i c_i}{n_m + n_i}$ the initial values for $t = 0$. Next, we denote $\tilde{\alpha} = \alpha \frac{n_m + n_i}{n_m n_i}$ the modified exchange coefficient and the characteristic time of exchange $T_{1/2} = \frac{\ln 2}{\tilde{\alpha}}$, which is the value used in practice as input value of the model. The discretisation scheme for both mobile (m) and immobile (i) concentrations is

$$(2.8) \quad C_{i,m}^{n+1} = (C_{i,m}^n - \bar{C}^n) e^{-\tilde{\alpha} \Delta t} + \bar{C}^n, \quad \bar{C}^n = \frac{n_m C_m^n + n_i C_i^n}{n_m + n_i},$$

where we omitted a symbol for mesh cell for readability and in the place of C_m^n , the result of previous advection calculation (C_k^{n+1} in (2.3)) in the current time step enters.

The expression (2.8) can be used for any time step, thus, comparing with the advection term alone, there is no more requirement on the time step of the model.

3. Discussion of the numerical behaviour. In general, the explicit upstream discretisation of the advection term brings a strong artificial dispersion, which depend on the relation of the mesh size, time step and fluid velocity, expressed by the Courant number C_r . We regard this effect from another side, that the numerical method calculates correct results of certian problem with a changed value of dispersion coefficient. Thus a possible way how to solve a given advection-dispersion problem is to use the reduced value $D' = D - D_{num}$, where D is the dispersion in the modelled physical system and D' is the dispersion as the input value of the model (see [7]). In our case, with no physical dispersion in the model, we have to approximate the value of D by the numerical dispersion (choice of Δx , Δt) in the calculation of the advection.

In general, for 3D problem and non-uniform mesh, it is difficult or impossible to exactly express the value of numerical dispersion. There exist a relation for one-dimensional problem with uni-directinoal fluid flow ([7])

$$(3.1) \quad D_{num} = \frac{1}{2}v\Delta x(1 - C_r),$$

which gives also a basic estimation for a more-dimensional case. Fulfilling the stability condition $C_r \leq 1$, we have the following limits for D_{num} :

$$(3.2) \quad D_{num} = 0 \quad \text{for } C_r = 1 \quad \text{and} \quad D_{num} \rightarrow \frac{1}{2}v\Delta x = D_{num}^{max} \quad \text{for } C_r \rightarrow 0.$$

With a given mesh and velocity, we can control the value of dispersion within the specified limits by a choice of time step. The limits can be modified by a choice of the mesh (Δx). The previous idea can be approximately generalized to a 3D model, where we consider some characteristic dimension of a cell instead of Δx .

To explain the substitution of the two processes of different matter – physical and numerical dispersion – we have to answer the following questions:

The first one is, for given D , how to construct the mesh such that $D_{num} \approx D$. This is not possible in general, but it can be done for advection-dominated problems satisfactorily. In practical problems, the dispersion value D can not be well measured, usually it is not given and the intensity of dispersion is verified by a model calibration. In our model, we check the mesh instead of D . Since the sensitivity of result to the value D is small and the other input values and measurement are known very roughly, it is not a critical matter to find an acceptable mesh.

Next, the non-uniform mesh and general field of velocity make the expression of the dispersion in the numerical model more complicated. We introduce a distribution of Courant number in a typical problem of “well-driven” flow (determined by drawing), with the mesh appropriatly constructed: finer around the wells and coarser near the boundary. The values for a realistic problem with 20 working wells and for a demonstrative problem with one well in the same domain are in the table 3.1.

It is clear to see that $C_r \ll 1$ for most of the computational domain, except of the cells very close to the wells. Thus, in fact, we apply a model with almost homogeneous dispersion coefficient, which can be roughly estimated by $\frac{1}{2}v\Delta x$.

TABLE 3.1

Distribution of Courant number for a typical remediation problem, with a mesh adapted to the velocity field (approx. 12000 cells).

interval of C_r	cell count in 20-wells problem	cell count in 1-well problem
(0.5, 1)	2 (0.02%)	2 (0.02%)
(0.25, 0.5)	32 (0.28%)	1 (0.01%)
(0.1, 0.25)	87 (0.72%)	12 (0.1%)
(0, 0.1)	98.98%	99.87%

4. Example and test problem. We consider a 1D problem in the interval $(0, L)$ with the following initial and boundary conditions (the domain is “clean” in the beginning and the solution of given concentration inflows from the left side) and material parameters:

$$(4.1) \quad \begin{aligned} c_m(x, 0) &= c_i(x, 0) = 0 \quad \forall x \in (0, L), \\ c_m(0, t) &= 1 \quad \forall t > 0, \\ n_m &= 0.2, \quad n_i = 0.2. \end{aligned}$$

The flow velocity is given by a Dirichlet problem with given values of the pressure head at the boundary points, $p_D(0) = 200\text{m}$ and $p_D(L) = 100\text{m}$. With a permeability $K = 1\text{m/d}$ and domain size $L = 1000\text{m}$, we calculate the Darcy velocity $q = 0.2\text{m/d}$ and the seepage velocity $v = 1\text{m/d}$ (the time is measured in days). The value of dispersion coefficient D will be considered according to the discretisation in the numerical calculation below and we will use a set of values of the exchange coefficient for comparisons (table 4.1).

4.1. Numerical solution. Using the 3D model with layer-ordered trilateral prismatic elements, we solve the above stated 1D problem on the mesh (figure 4.1) without any division in the rest directions. The lateral dimensions (b, h in the figure) are 50m and the total length 1000m is divided into 200 parts, which is 400 cells in total. The distance of neighbouring cell-centers is uniform, we can denote $\Delta x = 2.5\text{m}$.

The time step is chosen such that $C_r = \frac{1}{2}$, i.e. $\Delta t = 1.25\text{d}$. Thus, according to (3.1), our advection model solves the advection-dispersion problem with the coefficient value $D = 0.625\text{m}^2/\text{d}$. For the purpose of numerical-analytical comparison and display, the problem is solved in the time interval of 500 days: the “wave front” reach the half of the domain length and the whole concerned concentration curve can be observed. The rate of exchange is chosen through the values $T_{1/2}$ (table 4.1), such that the calculations cover the interesting behaviour in the interval $(0, \infty)$ of $T_{1/2}$.

4.2. Analytical solution. We use the analytical solution presented in [6], with minor modifications. First, the model is transformed to a dimensionless form

$$(4.2) \quad \beta \frac{\partial C_m}{\partial T} = -\frac{\partial C_m}{\partial X} + \frac{1}{P} \frac{\partial^2 C_m}{\partial X^2} + \omega(C_i - C_m),$$

$$(4.3) \quad (1 - \beta) \frac{\partial C_i}{\partial T} = -\omega(C_i - C_m),$$

where

$$(4.4) \quad X = \frac{x}{L}, \quad T = \frac{vt}{L}, \quad \beta = \frac{n_m}{n_m + n_i},$$

$$(4.5) \quad P = \frac{vL}{D} \text{ (Peclet number)} \quad \text{and} \quad \omega = \frac{\alpha L}{n_m v}.$$

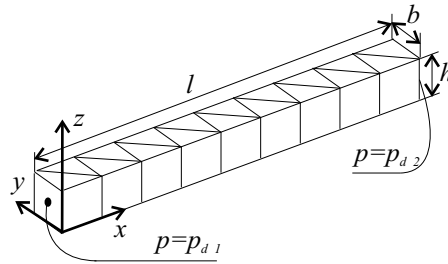


FIG. 4.1. The mesh for example calculation of 1D transport.

TABLE 4.1

Values of $T_{1/2}$ chosen for the example calculations and comparison of numerical and analytical solutions. The values of ω are appropriately derived for the use in the analytical solution.

$T_{1/2}$ [days]	ω (dimensionless)
∞ (turned-off exchange)	0
1000	0.3475
100	3.475
10	34.75
1	347.5
0	∞ (not calculated)

The concentration is transformed by $C_{m,i} = c_{m,i}/C_0$ with arbitrary value of characteristic concentration C_0 (we choose 1 in the appropriate dimension), this does not have any influence on the solution behaviour. The characteristic length L is considered as the dimension of problem domain. The initial and boundary condition of the problem (4.1) can be obviously directly applied in the transformed model. We apply no boundary condition for $x = L$, while there is no such boundary condition required in the numerical calculation and the presented analytical solution refers to the problem with semi-infinite domain (but only a part, given by the length L is concerned).

The solution $C_m(X, T)$ for above specified conditions is

$$(4.6) \quad C_m(X, T) = G(X, T) \cdot \exp\left(-\frac{\omega T}{\beta}\right) + \int_0^T G(X, \tau) \cdot \exp(-a - b) \cdot \left(\frac{1}{\beta} I_0(2\sqrt{ab}) + \sqrt{\frac{\tau}{\beta(1-\beta)(T-\tau)}} \cdot I_1(2\sqrt{ab})\right) d\tau,$$

where I_0 and I_1 are the modified Bessel functions of order zero and one respectively, $a = \frac{\omega\tau}{\beta}$, $b = \frac{\omega(T-\tau)}{1-\beta}$ and

$$(4.7) \quad G(X, \tau) = \frac{1}{2} \operatorname{erfc}\left(\frac{\beta X - \tau}{\sqrt{\frac{4\beta\tau}{P}}}\right) + \frac{1}{2} \exp(PX) \cdot \operatorname{erfc}\left(\frac{\beta X + \tau}{\sqrt{\frac{4\beta\tau}{P}}}\right)$$

is in fact the solution of a plain advection-diffusion problem. For advection-dominated problems (i.e. $P \gg 1$), the first term in (4.7) is dominant and the second one can be neglected (the second term provides to fulfil the boundary condition while the first term is a solution of a problem on a “both-side infinite” domain).

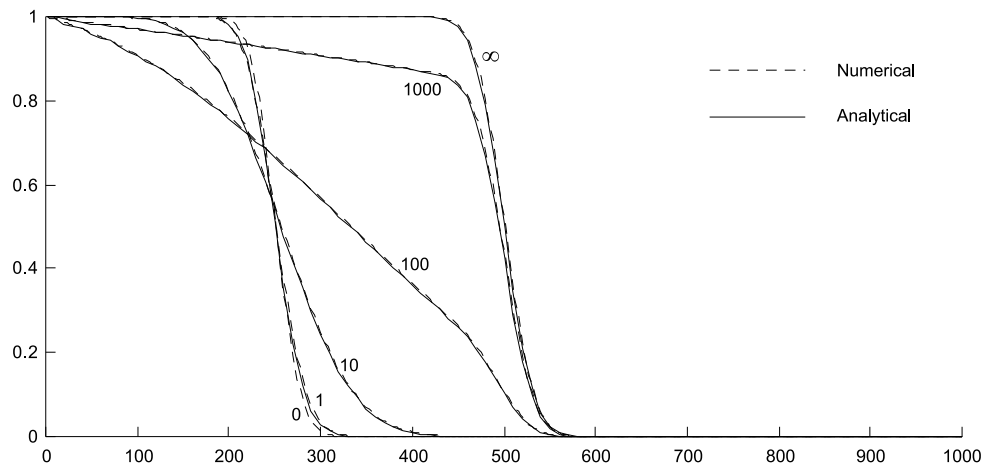


FIG. 4.2. Comparison of numerical and analytical solution of 1D problem of two-region nonequilibrium transport. The horizontal axis is the length in metres, the vertical axis is the dimensionless concentration. The curves are labelled by the values of exchange coefficient $T_{1/2}$ used for the calculations.

The calculation of the analytical solution requires numerical integration. It is interesting to remark, that the computational cost of the evaluation of the analytical solution is comparable with the numerical solution of the problem. The algebraical operations are relatively sensitive to computational errors (reductions of large values of the exponential functions), which causes some unnatural fluctuation of the displayed curves.

4.3. Comparison and discussion. For comparison, we transform the numerically solved problem to the dimensionless form and then we can directly draw graphs of the functions. The transformed parameters are

$$(4.8) \quad \beta = 0.5, \quad P = 1600$$

and the values of ω in the table 4.1. The resulting graphs are in the figure 4.2. The numerical and analytical solutions are almost identical in a graphical comparison. This accuracy is more than sufficient from a point of view of practical modelling, when the material parameters are known very roughly.

The important result of this study is that the proposed integration of the advection model (2.3) and the mobile-immobile exchange model (2.8) does not damage the overall approximation of the solved problem (2.1)-(2.2). We can easily accept this idea also for 3D problems with non-uniform mesh.

Next, the graphs show various interesting properties of the nonequilibrium transport. In the figure 4.2, the results for the limit values of $T_{1/2}$ (i.e. for no exchange and for an instant exchange) are displayed. The case of instant (equilibrium) exchange is governed by the advection-dispersion equation with a retardation factor $R > 1$ at the time-derivative term, which causes that the advection and dispersion run appropriately slower. Our results correspond with this model: since $R = \frac{n_m}{n_m + n_i} = 2$, the curve for instant exchange match the curve for no exchange except that it moves with a half velocity.

In the figure 4.3, we can observe the results for both mobile and immobile zone calculated by the numerical model. The continuous move of the contaminant from

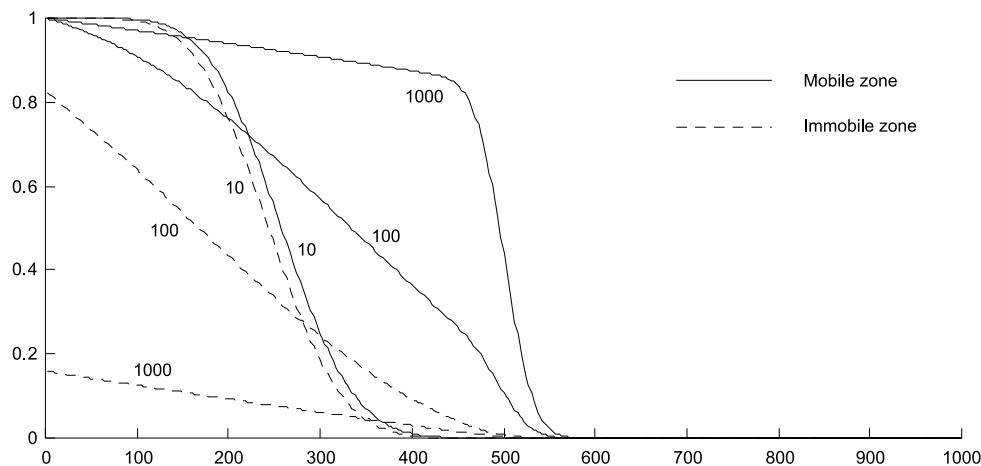


FIG. 4.3. Numerical solution of 1D problem of two-region nonequilibrium transport, the relation of mobile and immobile concentrations is demonstrated. The horizontal axis is the length in metres, the vertical axis is the dimensionless concentration. The curves are labelled by the values of exchange coefficient $T_{1/2}$ used for the calculations.

mobile to immobile zone is expressed in the difference between the two curves. The smaller is the time $T_{1/2}$, the quicker is the exchange and the closer is the process to an equilibrium.

5. Conclusion. We presented an efficient numerical approach for the two-region model of the solute transport in dual-porosity media. We concentrated on study of the effect of numerical dispersion in the upstream scheme and on the influence of mobile-immobile exchange. The numerical results on the example problem with appropriately chosen parameters correspond to the analytical solution, which confirm no undesirable interaction between the two processes in the model. A realistic remediation problem with physical dispersion in reasonable limits can be sufficiently accurately modelled by the presented approach.

REFERENCES

- [1] J. BEAR AND V. VERRUIJT, *Modeling groundwater flow and pollution*, D. Reidel Publishing Comp., Dordrecht, Holland, 1990.
- [2] K. H. COATS AND B. D. SMITH, *Dead end pore volume and dispersion in porous media*, Soc. Pet. Eng. J., 4 (1964), pp. 73-84.
- [3] C. GALLO, C. PANICONI AND G. GAMBOLATI, *Comparison of solution approaches for the two-domain model of nonequilibrium transport in porous media*, Adv. Water Resour., 19 (1996), pp. 241-253.
- [4] J. MARYŠKA, J. MUŽÁK, O. SEVERÝN AND J. ŠEMBERA, *Mathematical modelling of the inter-collector transfer of water contaminants*, Proceedings of ALGORITMY 2000, Slovak University of technology, Bratislava, Slovakia, pp. 120-129.
- [5] J. MARYŠKA, M. ROZLOŽNÍK AND M. TŮMA, *Mixed-hybrid finite-element approximation of the potential fluid-flow problem*, J. Comput. Appl. Math., 63 (1995), pp. 383-392.
- [6] N. TORIDE, F. J. LEIJ AND M. T. VAN GENUCHTEN, *A comprehensive set of analytical solutions for nonequilibrium solute transport with first-order decay and zero-order production*, Water Resour. Res., 29 (1993), pp. 2167-2182.
- [7] C. ZHENG AND G. D. BENNETT *Applied contaminant transport modeling*, Van Nostrand Reinhold, New York, 1995.